

Published in final edited form as:

Neuron. 2011 June 23; 70(6): 1165–1177. doi:10.1016/j.neuron.2011.05.023.

Defining the computational structure of the motion detector in *Drosophila*

Damon A. Clark¹, Limor Bursztyn², Mark Horowitz², Mark J. Schnitzer^{3,4,5}, and Thomas R. Clandinin^{1,*}

¹Department of Neurobiology, Stanford University, Stanford, California, USA

²Department of Electrical Engineering, Stanford University, Stanford, California, USA

³Department of Biological Sciences, Stanford University, Stanford, California, USA

⁴Howard Hughes Medical Institute, Stanford University, Stanford, California, USA

⁵Department of Applied Physics, Stanford University, Stanford, California, USA

SUMMARY

Many animals rely on visual motion detection for survival. Motion information is extracted from spatiotemporal intensity patterns on the retina, a paradigmatic neural computation. A phenomenological model, the Hassenstein-Reichardt Correlator (HRC), relates visual inputs to neural and behavioral responses to motion, but the circuits that implement this computation remain unknown. Using cell-type specific genetic silencing, minimal motion stimuli, and *in vivo* calcium imaging, we examine two critical HRC inputs. These two pathways respond preferentially to light and dark moving edges. We demonstrate that these pathways perform overlapping but complementary subsets of the computations underlying the HRC. A numerical model implementing differential weighting of these operations displays the observed edge preferences. Intriguingly, these pathways are distinguished by their sensitivities to a stimulus correlation that corresponds to an illusory percept, “reverse phi”, that affects many species. Thus, this computational architecture may be widely used to achieve edge selectivity in motion detection.

INTRODUCTION

Many animals, including insects, turn in response to wide-field visual motion cues, providing a behavioral read-out of the motion percept (Götz, 1964; Götz and Wenking, 1973; Hassenstein, 1951; Hassenstein and Reichardt, 1956; Hecht and Wald, 1934; Kalmus, 1949). A rich theoretical and experimental framework relates the spatiotemporal patterns of visual stimuli to the firing patterns of direction selective neurons and to optomotor behaviors (Buchner, 1976; Egelhaaf and Borst, 1989; Egelhaaf et al., 1989; Götz and Wenking, 1973; Haag and Borst, 1997; Hassenstein and Reichardt, 1956; Hausen and Wehrhahn, 1989; Reichardt, 1961; Reichardt and Poggio, 1976; Rodrigues and Buchner, 1984). These relationships can be compactly described by the spatial summation of local multiplication operations that compare visual contrasts over space and time, in a model known as the

*Correspondence should be addressed to T.R.C. (trc@stanford.edu).

COMPETING INTEREST STATEMENT

The authors declare no competing financial interests in this work.

Publisher's Disclaimer: This is a PDF file of an unedited manuscript that has been accepted for publication. As a service to our customers we are providing this early version of the manuscript. The manuscript will undergo copyediting, typesetting, and review of the resulting proof before it is published in its final citable form. Please note that during the production process errors may be discovered which could affect the content, and all legal disclaimers that apply to the journal pertain.

Hassenstein-Reichardt Correlator (HRC) (Hassenstein and Reichardt, 1956). Although neurons both upstream and downstream of the HRC have been studied in detail (Eckert, 1981; Haag and Borst, 1997; Hateren, 1992; Hausen, 1976; Joesch et al., 2008; Juusola et al., 1995; Katsov and Clandinin, 2008; Laughlin and Osorio, 1989; Rister et al., 2007; Van Hateren et al., 2005; Zhu et al., 2009), the neural implementation of the HRC itself remains elusive.

The HRC correlates light intensities between two points in space and time; an intensity deviation at one point is multiplied by an intensity deviation at a neighboring point at a later time (Figure S1A, B). By performing this operation twice, in anti-symmetric fashion, the signed output of the HRC provides information about the direction and speed of motion. This model was originally inferred from experiments using minimal motion signals comprising sequential changes in the brightness of two neighboring points in space that guided the turning behavior of a beetle, *Chlorophanus* (Hassenstein and Reichardt, 1956). In these experiments, each point in space could be made either brighter or darker than the background, producing four contrast combinations. Two of these combinations, where the two points change contrast in the same direction, with both becoming sequentially brighter or darker, can be referred to as “phi” stimuli. Such apparent motion signals caused the animal to turn in the same direction as the spatial sequence of contrast change at the two points. The other two contrast combinations, where the two points in space change their contrast in opposite directions, with one point becoming darker, and the other point becoming lighter, in either temporal order, are called “reverse phi” stimuli. Intriguingly, such signals caused the animal to turn in the opposite direction to that predicted by the spatial sequence of contrast change. This core result is captured by the sign-correct arithmetic multiplication imbedded in the HRC, representing increases in brightness as positive numbers, and decreases in brightness as negative numbers. Multiplying either two positive or two negative numbers produces positively signed outputs (and hence the same turning direction), while multiplying numbers of opposite sign produces negatively signed outputs (and a turn in the opposite direction) (Figure S1A). Sign-correct multiplication in neurons has long seemed implausible. It has thus been speculated, but never shown, that each sign pairing in the multiplication step might be implemented in a distinct computation (Hassenstein and Reichardt, 1956; Reiff et al., 2010).

Motion-evoked behaviors in *Drosophila* depend on R1-R6 photoreceptors, as well as their immediate post-synaptic targets, the lamina monopolar cells L1 and L2 (Heisenberg and Buchner, 1977; Katsov and Clandinin, 2008; Rister et al., 2007; Zhu et al., 2009). Recent electrophysiological studies have proposed that changes in contrast polarity are processed through two pathways, one devoted to detecting increases in brightness (an “ON” pathway), and the other devoted to detecting decreases in brightness (an “OFF” pathway) (Joesch et al., 2010; Reiff et al., 2010). In these studies, blocking synaptic output from L1 or L2 caused the reciprocal loss of responses of a subset of lobula plate tangential cells (LPTCs) to either light or dark moving edges, respectively (Joesch et al., 2010). However, the computational mechanism by which this selectivity emerges is unclear. Here we use minimal motion signals, in combination with genetic manipulations of the input pathways to the HRC, *in vivo* calcium imaging, and numerical modeling to examine the computational structure of the HRC with respect to its inputs from L1 and L2.

RESULTS

Measuring the delay filters of the HRC for turning behavior in *Drosophila*

To examine the inputs to the HRC, we constructed an apparatus that would allow us to easily display complex visual stimuli to a stationary fly while monitoring the circuit’s output, the fly’s turning behavior. We allowed the fly to walk in place on a spherical

treadmill while its thorax was held in place. We presented each fly with broad-field visual stimuli (Figure S1C) and used the motion of the ball as a measure of the animal's turning (Figure 1A, B; (Buchner, 1976; Seelig et al., 2010)). In response to rotating square wave gratings, flies in this apparatus produced turning responses comparable to those seen in other experimental systems (Figure 1B, C; (Tammero et al., 2004)).

We sought to characterize the wild-type HRC over a wide range of contrast changes and input delays. To do this, we generated a stimulus comprising spatially periodic bar pairs, in which we varied the contrast of each bar independently and randomly in time while monitoring the fly's turning response (Figure 2A; (Marmarelis and McCann, 1973)). Each bar subtended 2° in azimuth. As the spatial acceptance angle of the *Drosophila* ommatidium is 5.7° , and the separation between adjacent ommatidial centers is 5.1° (Stavenga, 2003), by design this visual display stimulated no more than two adjacent points in space. In many cases, both points will fall within a single receptive field. Thus, this stimulus represents a minimal motion signal, which should produce small turning responses predicted by the HRC in a manner dependent on multiplication of the contrasts of the two bars (Figure 2B). While flies did not respond to either bar's intensity individually (Figure S2A, B), they did respond to the joint distribution of the two bars' intensities in time, characterized by a two dimensional kernel (Figure 2C, D). As expected, this kernel had the form predicted by the HRC, with strong responses corresponding to sequential contrast changes at short temporal offsets. From this two-dimensional filter and a simple HRC model (Egelhaaf et al., 1989), we determined the shape of two filters: the delay filter, which determines the temporal correlation time in the model, and the behavioral response filter, which takes into account the delay and dynamics of the fly's response to perceived motion (Figure 2E). The delay filter under these dynamical conditions peaked near 25 ms, close to measurements of the delay based on electrophysiological studies in other flies (Harris et al., 1999). The behavioral response filter also matches known fly response times (Theobald et al., 2010). We compared the mean fly response to the response predicted by the HRC kernel, and found that the relationship was linear, consistent with flies responding to the product of contrasts, as predicted by the HRC (Figure 2F; (Hassenstein and Reichardt, 1956; Heisenberg and Buchner, 1977)). We note that, as expected for such a weak motion stimulus, fly rotation is strongly dominated by stimulus-independent noise under these conditions, and that this kernel predicts only a small fraction ($\sim 1\%$) of the variance in mean turning behavior. Taken together, the aggregate properties of the fly's rotational responses to motion in our apparatus match those predicted by the HRC.

Behavioral responses to motion mediated by L1 and L2 are selective for contrast polarity

Most motion stimuli comprise the simultaneous movement of both light and dark edges, defined respectively by a transition from dark to light (the "light" edge) and a transition from light to dark (the "dark" edge). We first examined turning responses to edges of each individual type, in which a single edge type rotates about the fly. Control flies turned in a direction-selective manner in response to the motion of each edge type individually, with approximately equal magnitude, as well as to both edge types moving simultaneously in a rotating square wave grating (Figure 3; see Figure S3A for diagrams of the stimuli). Using a genetic approach, we then disrupted synaptic transmission in either L1 or L2, or both, and examined the flies' responses (see Figure S3B for drivers). As expected from previous work, silencing both cells' synapses using the genetically encoded inhibitor of endocytosis, *shibire^{ts}*, strongly suppressed responses to wide field motion ((Rister et al., 2007); Figure S3C). Silencing only L2, leaving L1 intact, slightly reduced responses to dark edges but left responses to light edges and cylinders largely intact (Figure 3A, C, D, F, G, I). By contrast, silencing only L1, leaving L2 intact, had a strongly differential effect, almost eliminating

responses to light edges, but leaving responses to dark edges and cylinders intact (Figure 3B, C, E, F, H, I).

These single edge stimuli were necessarily associated with global changes in light levels, which could impact behavioral response indirectly. To examine responses to specific edge types without causing such global changes, we devised an equiluminant stimulus in which light and dark edges moved in opposite directions at equal speeds, simultaneously (Figure S3A). Control flies presented with this stimulus displayed only a small response, turning slightly in the direction of the light edge movement, indicating that the neural pathways activated by moving light and dark edges are normally summed so as to render them almost balanced in strength (Figure 3J-L). When L2 was silenced, leaving only L1 intact, flies turned in the direction of the light edges (Figure 3J, L). Conversely, when L1 was silenced, flies turned in the direction of the dark edges (Figure 3K, L). We infer that these turning responses reflect unbalanced motion signals produced by light and dark edges, consistent with the edge selective responses observed in the L1 and L2 pathways. As expression of the L1a driver was not completely specific to L1, we obtained similar results with an alternate L1 driver, L1b (Figure S3D). Moreover, edge selectivity was not strongly dependent on luminance; when luminance was decreased tenfold, the L1 and L2 pathways displayed approximately the same preference for light and dark edges (Figure S3E). Taken together, these experiments indicate that L1 and L2 are preferentially required for to process the motion of light and dark edges, respectively.

L1 and L2 axon terminals respond similarly to light and dark flashes

These disparate responses to moving edges could be the result of differential activation of L1 and L2 by positive and negative contrasts (Joesch et al., 2010). We sought to test this hypothesis by examining calcium signals in L1 and L2 axon terminals. L1 axons terminate in the M1 and M5 layers of the medulla, while L2 terminates in M2 ((Fischbach and Dittrich, 1989); Figure 4A, B). The light-evoked responses of L2 terminals have been described by measuring changes in intracellular calcium concentrations using the genetically encoded indicator TN-XXL (Mank et al., 2008; Reiff et al., 2010). These previous studies described the responses of L2 termini to long presentations of light, interleaved with darkness, and observed more prominent responses to the offset of light than to the onset. Accordingly, prior work had concluded that L2 is “half-wave rectified”, responding primarily to darkening (Reiff et al., 2010). We used two-photon microscopy and TN-XXL to record changes in calcium concentrations at L1 and L2 axonal terminals in response to restricted-wavelength visual stimuli (Figure S4A,B,C). By applying bright and dark flashes, we reproduced the previously reported responses of L2 (Figure 4C, Figure S4D). Extending these studies to L1 revealed that the terminal of L1 in the M1 layer of the medulla responds similarly to that of L2 to alternating light and dark epochs, showing increases in intracellular calcium levels during dark periods and decreases during light periods (Figure 4C, S4E). The M5 terminal of L1 responded with the same polarity, but with an attenuated strength (Figure 4C).

L1 and L2 axon terminals respond to both moving light and dark edges

We next examined the responses of both L1 and L2 to a moving light edge, moving at 80 degrees/s, across a dark background. After the light edge passed, the screen was white for four seconds, following which a dark edge moved across, also at 80 degrees/s, in the same direction. Under these conditions, the trace of the response to this stimulus showed the cellular response to both edge types as sequential events (Figure 4D, Figure S4F). The calcium signal in the L1M1 terminal decreased in response to the light edge passing, and remained low until the dark edge passed, when it increased transiently before returning to baseline. The L1M5 terminal displayed a broadly similar response, but with a smaller

amplitude, consistent with the difference in flash responses. The L2 terminal displayed a transient decrease in calcium in response to the light edge and a transient increase in response to the dark edge. Importantly, the calcium signals of both L1 and L2 terminals showed responses to both edge types, with comparable magnitudes for L1 and a more pronounced response to dark edges for L2 (Figure 4E). Thus, although the L1 and L2 terminals respond with different long time scale kinetics, traces from both neurons clearly contained information about both edge types.

L1 and L2 axon terminals respond linearly to changes in contrast

Signal rectification is thought to be a critical component of the HRC (Hassenstein and Reichardt, 1956). In one implementation of this rectification, an input channel could preferentially transmit information about contrast increases or decreases, but not both. Indeed, recent work proposed that calcium signals in L2 terminals are half-wave rectified to respond only to decreases in brightness, not increases (Reiff et al., 2010). To quantitatively compare the responses of L1 and L2 to positive and negative changes in contrast, we sought to characterize these responses across a range of contrasts, at timescales relevant to motion detection, under continuous illumination. To do this, we presented flies with a full-field, random intensity stimulus, with a standard deviation of 35% contrast about a mean luminance, and a 200-ms correlation time. The relatively fast intensity changes in this stimulus effectively prevent strong adaptation from taking place on time scales longer than 200 ms. As expected, intense periods of illumination prompted a reduction in intracellular calcium levels in both cell types. Periods of decreased illumination induced an increase in calcium levels (Figure 5A). Using this stimulus, the maximum correlation between contrast and calcium signal occurred with a delay of 80-130 ms (data not shown), consistent with the indicator kinetics, the imaging frame rate, and our observations of the flash responses. To examine whether responses to contrast increases were equal and opposite to contrast decreases, we plotted the calcium-indicator ratio against the contrast presented 100 ms earlier for all three axon terminals (Figure 5B). The output of all three terminals varied linearly with the delayed input contrast. A purely linear function accounted for 97% and 89% of the mean delayed response variance of the L1 signals in M1 and M5; a quadratic term accounted for less than 1% of additional variance in each case. Similarly, a purely linear function accounted for 99.6% of the variance in L2 responses, while adding a quadratic term accounted for less than 0.1% of additional variance.

As a second approach to measuring response linearity, we fit a linear – non-linear (LN) model to the calcium response of these cells, as a function of contrast history, following methods used extensively to characterize responses in vertebrate retina (Figure S5A, B; (Baccus and Meister, 2002; Chichilnisky, 2001; Sakai et al., 1988)). These linear kernels were strongly predictive of the average responses of L1 and L2 to these stimuli (Figure S5A, B). Furthermore, plots of the actual responses versus those predicted by these filters were highly linear (Figure S5C). Thus, we found no evidence that edge selectivity could emerge simply through the directed transmission of contrast increases through L1 and contrast decreases through L2.

Drosophila implements all four unit computations of the HRC

A biologically plausible model for the HRC has been proposed to include four independent computations of the multiplication events that underlie responses to sequential presentation of two bright, two dark, bright then dark, and dark then bright bar pairs (Hassenstein and Reichardt, 1956). However, whether these four putative computations are actually independently implemented, and whether fruit fly behavior can be elicited by each of the unit computations, is unknown. We therefore presented flies with a spatially periodic pattern of identical, separated pairs of adjacent bars, 5° in width, to generate a turning signal based

on the order in which the bars changed intensity. As expected, flies turned in the direction predicted by the order and direction of the change in contrast when neighboring bars turned sequentially brighter or darker (“phi” stimuli; Figure 6A-C). The HRC predicts an opposite response to reverse phi stimuli, the sequential brightening of one bar, followed by darkening of the second bar (and *vice versa*) (Anstis, 1970; Hassenstein and Reichardt, 1956). Accordingly, flies turned in the opposite direction to such sequential presentations (Figure 6A-C). The magnitude of the response remained unchanged even when the delay between when the first bar turned on relative to the second bar was one second (Figure 6D,E). This means that the delay filter arm of the wild-type HRC can transmit information about contrast for at least one second. Thus, fruit flies generated appropriate behavioral responses to all four signed computations of the HRC.

L1 and L2 pathways implement different subsets of the HRC unit computations

We next examined how the edge selectivity of the L1 and L2 pathways might be achieved through the computations that underlie the HRC. To do this, we examined responses to sequential bar stimuli in flies in which either only L1 or only L2 remained functional (Figure 7). Our initial prediction was that the L1 pathway, which responded more strongly to light edges, should respond preferentially to bright-bright stimuli over dark-dark stimuli. Conversely, the L2 pathway, which responded almost exclusively to dark edges, should respond preferentially to dark-dark stimuli relative to bright-bright stimuli. However, we observed that flies having only L1 or only L2 intact displayed strong responses to both sequential bright-bright and dark-dark stimuli (Figure 7A-F; Figure S6A,B).

The two reverse phi stimuli, however, evoked differential, complementary responses in the two pathways (Figure 7G-L; Figure S6C,D). Flies bearing only an intact L1-pathway lost responses to the bright-dark stimulus, but retained a normal response to a dark-bright stimulus (Figure 7G, I, J, L). Conversely, flies bearing only a functional L2-pathway responded strongly to a bright-dark stimulus, but only weakly to the dark-bright stimulus (Figure 7H, I, K, L). Together, these results demonstrate that both L1 and L2 convey information about both positive and negative contrast changes to motion detection, and that a key difference between the two pathways lies in their responses to reverse phi signals.

Pathway specific processing of reverse phi signals is sufficient to produce edge selectivity

The apparent selectivity of L1 and L2 pathways for reverse phi motion is counterintuitive if one considers such stimuli to be purely artificial. We therefore considered the possibility that they might, in fact, be important to normal motion vision. A moving light or dark edge produces a change in two neighboring points in space at subsequent points in time, creating changes in pair-wise space-time correlations (Figure 8A). One pair-wise correlation corresponds to that associated with phi motion, either a sequential lightening or darkening of the two inputs to a motion detector. Interestingly, a second pair-wise correlation is also generated in the opposite direction, corresponding to a reverse phi signal. The reverse phi signal is specific to the type of edge, with light edges associated with dark-bright reverse phi, and dark edges associated with bright-dark reverse phi. Intriguingly, animals bearing only a single functional L1 or L2 neuron-type retained only the reverse phi signal appropriate to the edge type for which they are behaviorally selective.

We therefore considered whether these reverse phi correlations could be important for edge selectivity. To do this, we created a weighted quadrant model. We simulated an array of HRCs with response properties to phi and reverse phi stimuli that were appropriate to either the L1 or L2 pathway, and examined their edge selectivity. In particular, we constructed our model using the measured weightings of the unit computations of the HRC (Figure 7). That

is, the only difference between the two pathways in our model was the differential weightings of the four unit multiplications of the filtered intensity input. In constructing the model, we also incorporated the following assumptions. First, as L1 and L2 pathways are thought to be completely sufficient for motion detection (Rister et al., 2007), our model included only these inputs. Second, we used both our measured delay filter and the behavioral filter, taken from measurements of wild-type flies (Figure 2, see Supp. Methods). Third, while the kinetics of genetically encoded calcium indicators are too slow to allow us to directly measure a physiological filter for L1 and L2, electrical recordings in LMC cell bodies made in blowfly at similar intensities to our experiments have shown that LMCs act as high-pass or band-pass filters, emphasizing changes in contrast and suppressing absolute contrast on time scales longer than ~50-100 ms (Juusola et al., 1995; Laughlin et al., 1987). The high-pass filter incorporated into our model was therefore made to be consistent with these measurements. We validated our model by showing that it responded to the sequential bar stimuli in the same proportions as the corresponding silenced flies; this result is by construction (Figure S7A). A version of the model including both pathways, representing a wild-type fly, when subjected to random Gaussian contrast bar pairs (Figure 2A), yielded filters that closely resembled those measured in Figure 2 (Figure S7B,C).

Using this model, we then calculated the predicted responses of L1 and L2 pathways to light and dark edges, and compared the edge selectivity in those responses to the actual edge selectivity observed in each pathway. We defined edge selectivity as the integrated light edge response minus the integrated dark edge response, divided by their sum. The modeled selectivity using our differentially weighted, asymmetric HRC array was close to the measured selectivity, with the L1 pathway predicted to be slightly more selective than we observed, and the L2 pathway predicted to be slightly less selective (Figure 8C). These small differences could reflect small measurement errors in the relative weightings of the unit computations, as the model can produce more, or less, selective outputs depending on the exact values used (data not shown). Simply weighting the phi stimuli equally, while differentially weighting the reverse phi stimuli is sufficient to produce edge selectivity (data not shown). Moreover, the edge selectivity observed using this model was relatively insensitive to many other parameters of the model, as long as the high pass filters operated under relatively short timescales (<100 ms; data not shown). Thus, these simulations demonstrate that organizing the HRC into an asymmetric, weighted architecture is sufficient to produce appropriate edge-selective responses in the L1 and L2 pathways.

DISCUSSION

In this work, we examined the structure of the HRC underlying turning behavior by manipulating its inputs. Our results demonstrate that behavioral responses to motion signals are edge polarity selective, and that L1 and L2 provide inputs to pathways that are differentially tuned to the motion of light and dark edges, respectively. Using quantitative measurements of calcium signals in L1 and L2 axon terminals, we found that these two cells both respond to increases and decreases in brightness. Thus, their specialization for moving light and dark edges lies downstream of these signals, in the underlying neural circuits to which they connect. Using minimal motion stimuli, we then demonstrate that phi and reverse phi computations are grouped together in each pathway so as to achieve edge selectivity. Finally, by constructing an asymmetrically weighted model of the HRC, we demonstrate that this organization is sufficient to produce edge selective motion processing. As reverse phi signals are the critical component of this model, and correspond to visual illusions perceived by many animals, we propose that these signals are likely to play a widespread role in the emergence of edge selectivity in motion detection.

Characterizing the HRC in *Drosophila*

The HRC is thought to underlie motion vision in all insects (reviewed in (Borst, 2009; Borst et al., 2010)), and there is considerable interest in applying the genetic tools available in *Drosophila* to dissecting the neural circuitry that implements this paradigmatic computation. However, a number of important parameters of this model had not previously been measured in this animal. To extract the form of the HRC delay filter, we combined minimal motion stimuli with linear response analysis, and were able to determine a behavioral delay filter whose time course closely parallels previous measurements made in other species using electrophysiological recordings from direction-selective neurons (Harris et al., 1999; Marmarelis and McCann, 1973). Moreover, using sequential bar pair stimuli, we found that this insect is capable of all four unit computations predicted in the original “four-quadrant multiplication” model (Hassenstein and Reichardt, 1956). Finally, as had previously been reported using electrophysiological recordings of direction-selective neurons (Joesch et al., 2010), we also found that behavioral responses to motion are mediated by two pathways that are individually selective for the motion of bright edges and dark edges. We anticipate that these measurements and stimuli will provide a strong experimental basis for analyzing behavioral responses in animals in which the activities of many neurons involved in motion detection have been altered, and will allow precise assignments of computational function to these different cells.

Integrating imaging and electrophysiological studies of the responses of L1 and L2

Consistent with a sign-inverting, histamine-gated chloride channel mediating L1 and L2 responses to photoreceptor input, we observed that increases in contrast caused decreases in intracellular calcium signals in both axonal terminals of L1, and the terminal of L2. These three terminals displayed remarkably linear responses to dynamical contrast changes, but different kinetics in response to prolonged stimuli. Such kinetic differences have not been noted in the electrophysiological recordings of LMCs (Juusola et al., 1995; Laughlin et al., 1987), but may be related to differential adaptation in each neuron type. In particular, the L2 terminal adapted to long presentations of a contrast signal, returning to near baseline, while the L1 M1 terminal retained low calcium levels throughout a four second light presentation, then returned to baseline with a small overshoot when the light was removed. The L1 terminal in M5 showed a response that was qualitatively similar to, but attenuated, as compared to the M1 response.

Several previous studies have used electrophysiological techniques and linear response analysis to examine the functional properties of laminar cells in larger flies (Juusola et al., 1995; Laughlin et al., 1987). They have found that in dim conditions, laminar cell membrane potential, measured at the cell body, tends to follow the contrast itself, while under bright conditions, laminar cells respond most to changes in contrast. Thus, the filters measured in these electrophysiological studies are on the timescale of 50ms, with the responses to light steps occurring with a timescale on the order of <100ms. We infer, then, that under the bright conditions of our imaging and behavioral experiments, a step change in contrast elicits a transient electrical change in LMC membrane potential, lasting less than 100 ms, following which the cell returns to near baseline potential. In contrast, the calcium responses we measure in axonal terminals can persist for seconds. This difference is not solely due to the kinetics of the calcium reporter, since the time scales can be much longer than the off rate of the indicator (Reiff et al., 2010). The difference could reflect processing that takes place within the axon, but it seems unlikely that such long time scales are useful in transmission of information relevant to motion detection. Instead, they likely reflect adaptation processes occurring at the synapse.

Rectification emerges downstream of L1 and L2 terminals

A central aspect of implementing arithmetic multiplication in the brain is thought to be “half-wave rectification” of the inputs to each multiplier (Hassenstein and Reichardt, 1956). That is, because it is difficult to conceive of how a single synapse or circuit could implement sign-correct multiplication of all possible combinations of positive and negative inputs, it seems plausible that multiplied inputs would be rectified so that each sign pairing could be multiplied independently. Given the apparent need for rectification, a key question becomes where these rectification events get implemented within the motion detection circuitry.

Recent work used imaging studies of calcium signals in the L2 axon terminal to argue that the output of this cell was half-wave rectified such that it primarily transmitted information about decreases in brightness (Reiff et al., 2010). In particular, when these cells were exposed to long periods of darkness, followed by light flashes, these axon terminals responded strongly to the onset of darkness, but only relatively weakly to the onset of light. Our imaging data, using the same calcium indicator, support the existence of some asymmetry under similar conditions. However, our data also demonstrate that under continuous dynamical illumination, the calcium signal in this cell varies nearly linearly with contrast. In addition, if the output of this cell were rectified, then flies bearing only active L2 cells should be unable to respond normally to any visual stimulus whose content requires information about increases in brightness (since a rectified L2 output cannot transmit this information). Our behavioral studies demonstrate that this is not the case: flies with only active L2 cells respond normally to one of the two reverse phi stimuli, a signal whose central component is brightening at one point in space, as well as to a normal phi stimulus consisting of brightening in two points in space. Finally, a reasonable prediction from a model in which L2 outputs are half-wave rectified would be that the outputs of the L1 cell would also be half-wave rectified in the opposite direction. However, both our imaging data, and our behavioral studies, demonstrate that L1 conveys information about both brightening and darkening to the HRC. Thus, while our model of the HRC does require rectification, this rectification is not implemented within L1 or L2, and therefore must be implemented in the circuitry downstream of these neurons. Moreover, these observations argue strongly that the fly visual system is not organized into ON and OFF pathways in which L1 and L2 pathways transmit information only about increases and decreases in contrast, respectively, as has been proposed (Joesch et al., 2010).

Edge selectivity emerges from a weighted organization of the HRC

Previous studies based on behavioral and electrophysiological approaches have suggested a number of possible configurations of motion detection pathways (Egelhaaf et al., 1989; Hassenstein and Reichardt, 1956; Reiff et al., 2010). Our results define this computational architecture with respect to its input pathways (Figure 8B). As the calcium signals detected in L1 and L2 are not themselves rectified, and as both pathways contribute to behavioral responses that involve both lightening and darkening, these pathways must each feed into partial HRCs, which perform computations with information about both intensity increases and decreases. The HRC downstream of L1 computes responses to both sequential brightening and darkening. However, it also computes responses to the sequential dark-bright stimulus combination, the reverse phi percept that is specifically associated with light edges. Incorporating this additional computation tunes behavioral response to moving light edges. The HRC downstream of L2 also responds to sequential darkening and lightening, as well as to the bright-dark combination, and thus can use the appropriate reverse phi signal to become selective for behavioral responses to moving dark edges. Thus, each pathway computes a subset of HRC operations to assemble a filter tuned to a specific type of moving edge. This architecture provides a computational mechanism for the specificity of these two

input channels (Joesch et al., 2010), while the intact circuit would still respond appropriately to all four paired correlations that mediate turning responses in wild-type flies.

This model uses the intrinsic correlations present in light and dark edges to create selective filters by differentially weighting the four unit computations of the HRC. Because the four pair-wise contrast combinations are present in different proportions in light edges and dark edges, and particularly because the two reverse phi combinations are each associated with a single edge type, a circuit can respond selectively to an edge by appropriately weighting reverse-phi signals. We have defined the four computations here by the contrasts of the first and second bars in the bar pair experiments to which they correspond. However, we note that because the four multiplications act on filtered versions of the contrast input, for quickly varying inputs they will not always correspond to the instantaneous contrasts. Importantly, if the non-delayed filter were to transmit too much of the DC component of the intensity, the result would be that the two pathways would individually promote turning responses to static spatial gradients, since the static gradient would be interpreted as a reverse phi in one direction. As we have not observed such behavior from L1 and L2 silenced flies in our apparatus (data not shown), we included a high passing filter in the model (Figure 8B; compare with Figure S1A, B), so as to cause the signal on the un-delayed arm of the HRC to fall to zero over a short timescale.

By segregating the unit computations of the HRC into two pathways, it is possible to weight the individual computations differently for distinct behaviors, providing an explanation for the behavioral specializations in input pathways that were noted previously (Duistermars et al., 2007; Katsov and Clandinin, 2008). This flexibility to independently weight the outputs of each unit computation also provides a possible explanation for the differences in selectivity seen between our behavioral studies and the electrophysiological studies of single direction-selective neurons (Joesch et al. 2010). That is, since behavior measures the output of an entire circuit, it is formally possible that the particular neurons examined electrophysiologically are a subset of the neurons contributing to the behavior, and other contributing neurons are less edge polarity selective. In addition, it is possible that the precise structure of the stimulus used may also play a role, as our behavioral stimuli are notably faster and more frequent than the stimuli used during previously published recordings (Joesch et al., 2010). Finally, the segregation of light and dark edge information has been suggested to be involved in fine feature detection in insects (Nordström and O'Carroll, 2009; Wiederman et al., 2008).

These results are also broadly consistent with previous studies that have examined the behavioral effects of manipulating various lamina neuron subtypes (Joesch et al., 2010; Katsov and Clandinin, 2008; Rister et al., 2007; Zhu et al., 2009). Rister et al. (2007) demonstrated that L1 and L2 are necessary and individually sufficient for motion vision; that L1 and L2 feed into motion detectors with similar temporal properties; and that at low contrast, L1 mediates back to front motion detection while L2 mediates front to back motion detection. Our behavioral observations and modeling studies are consistent with this work, but we did not test the low contrast conditions under which the previously reported direction-selectivity for these pathways arises. We note that the rescue experiments, which demonstrated the sufficiency of L1 and L2 pathways for motion detection, examined responses to cylinders, which include all four unit computations of the HRC (Rister et al., 2007). It is therefore possible that these studies rescued only a subset of the computations we find in each pathway. Katsov and Clandinin (2008) showed that the L2 pathway could differentially modulate direction selective translational and rotational walking behaviors. The stimuli used in these experiments were symmetric with respect to light and dark edges, and thus did not examine possible independent roles for these edge types. Finally, a prominent role for L4 in the HRC has also been proposed (Zhu et al., 2009); as this cell is

thought to act downstream of both L2 and amacrine cells, our work has not examined its function.

The role of reverse phi in motion detection

Our data demonstrate that reverse phi signals have both specific neural representations and also functional utility. Intriguingly, neurons in the cortex and lateral geniculate nucleus of vertebrate visual pathways respond to phi and reverse phi motion (Krekelberg and Albright, 2005; Livingstone et al., 2001). Humans, and other primates, among other animals, respond to reverse phi illusions (Bours et al., 2007; Bours et al., 2009; Livingstone et al., 2001), and in humans as in flies, the responses to phi and reverse phi are of similar magnitude. Furthermore, in humans, reverse phi percepts share many properties with motion after-effects (Bours et al., 2007). Theoretical considerations have further suggested that reverse-phi responses must mix ON and OFF visual pathways at an early stage to achieve the observed cellular sensitivities (Mo and Koch, 2003). Intriguingly, cells in the monkey striate cortex have also been reported to respond selectively to edge polarity (Schiller et al., 1976). Thus, we speculate that reverse phi, rather than being illusory, contributes to perception of moving edges of specific polarity. As edge detecting simple cells represent a fundamental unit of computation in vertebrate visual systems (Hubel and Wiesel, 1968; Jones and Palmer, 1987), and edges represent independent components of the visual scene (Bell and Sejnowski, 1997), our results suggest that edge polarity detection is an additional, important feature of visual motion processing.

EXPERIMENTAL PROCEDURES

The Gal4 drivers L1a (split Gal4, from (Gao et al., 2008)), as well as L1b (c202a-Gal4 from (Rister et al., 2007)), and L2 (21DGal4, from (Rister et al., 2007)) were used to express *shibire^{ts}* and TN-XXL in L1 and L2 neurons for behavior and imaging experiments. Visual stimuli were updated at a rate of 240Hz by optically coupling the output of a digital light projector to 3 (for behavioral experiments) or 1 (for imaging experiments) 4×4mm coherent fiber-optic bundles, which were placed near the fly's eye, achieving a spatial resolution of ~1 pixel/degree.

Behavioral experiments were performed with tethered flies walking on an air-suspended 6.13mm polypropylene ball (Buchner, 1976; Seelig et al., 2010). Ball position and rotation around 3 axes was measured using 2 optical USB pen mice. All behavioral experiments lasted 20 minutes and were performed at 34°C, the restrictive temperature for *shibire^{ts}*. Stochastic stimuli were presented continuously, while non-stochastic ones were randomly interleaved, with periods of gray in between stimuli.

Flies for imaging were cold-anaesthetized before being mounted in a small hole, where the back of their head capsule could be removed. We used a two-photon microscope to obtain ratiometric measurements of TN-XXL emissions from labeled cell types while presenting visual stimuli in a narrow spectral band with a central wavelength of 575nm. Imaging experiments typically lasted 60 minutes for each fly. See Supplementary Material for complete methods.

Supplementary Material

Refer to Web version on PubMed Central for supplementary material.

Acknowledgments

The authors thank Axel Borst, Chi-Hon Lee, Daryl Gohl, Mathias Wernet, and Marion Silies for fly stocks, and Bob Schneeveis for assistance in constructing the behavioral rig. The authors would also like to thank James Fitzgerald and Tony Movshon for helpful discussions, and Liqun Luo, Miriam Goodman, Saskia de Vries, Daryl Gohl, and Marion Silies for comments on the manuscript, and Sheetal Bhalerao for aid with dissections. This work was supported by a Jane Coffin Childs Postdoctoral fellowship (D.A.C.), a Fulbright Science and Technology Fellowship and a Stanford Bio-X SIGF Bruce and Elizabeth Dunlevie Fellowship (L.B.), the W.M. Keck Foundation (MH, MJS, TRC), and NIH Director's Pioneer Awards to M.J.S (DP10D003560) and T.R.C. (DP0035350).

References

- Anstis S. Phi movement as a subtraction process. *Vision Research*. 1970; 10:1411–1430. [PubMed: 5516541]
- Baccus S, Meister M. Fast and slow contrast adaptation in retinal circuitry. *Neuron*. 2002; 36:909–919. [PubMed: 12467594]
- Bell A, Sejnowski T. The “independent components” of natural scenes are edge filters. *Vision Research*. 1997; 37:3327. [PubMed: 9425547]
- Borst A. Drosophila's view on insect vision. *Current Biology*. 2009; 19:R36–R47. [PubMed: 19138592]
- Borst A, Haag J, Reiff DF. Fly motion vision. *Annual review of neuroscience*. 2010; 33:49–70.
- Bours R, Kroes M, Lankheet M. The parallel between reverse-phi and motion aftereffects. *Journal of vision*. 2007; 7
- Bours R, Kroes M, Lankheet M. Sensitivity for reverse-phi motion. *Vision Research*. 2009; 49:1–9. [PubMed: 18848956]
- Buchner E. Elementary movement detectors in an insect visual system. *Biological Cybernetics*. 1976; 24:85–101.
- Chichilnisky E. A simple white noise analysis of neuronal light responses. *Network: Computation in Neural Systems*. 2001; 12:199–213.
- Duistermars B, Chow D, Condro M, Frye M. The spatial, temporal and contrast properties of expansion and rotation flight optomotor responses in *Drosophila*. *The Journal of experimental biology*. 2007; 210:3218. [PubMed: 17766299]
- Eckert H. The horizontal cells in the lobula plate of the blowfly, *Phaenicia sericata*. *Journal of Comparative Physiology A: Neuroethology, Sensory, Neural, and Behavioral Physiology*. 1981; 143:511–526.
- Egelhaaf M, Borst A. Transient and steady-state response properties of movement detectors. *Journal of the Optical Society of America A*. 1989; 6:116–127.
- Egelhaaf M, Borst A, Reichardt W. Computational structure of a biological motion-detection system as revealed by local detector analysis in the fly's nervous system. *Journal of the Optical Society of America A*. 1989; 6:1070–1087.
- Fischbach K, Dittrich A. The optic lobe of *Drosophila melanogaster*. I. A Golgi analysis of wild-type structure. *Cell and Tissue Research*. 1989; 258:441–475.
- Gao S, Takemura S, Ting C, Huang S, Lu Z, Luan H, Rister J, Thum A, Yang M, Hong S. The neural substrate of spectral preference in *Drosophila*. *Neuron*. 2008; 60:328–342. [PubMed: 18957224]
- Götz K. Optomotorische untersuchung des visuellen systems einiger augenmutanten der fruchtfliege *Drosophila*. *Biological Cybernetics*. 1964; 2:77–92.
- Götz K, Wenking H. Visual control of locomotion in the walking fruitfly *Drosophila*. *Journal of Comparative Physiology A: Neuroethology, Sensory, Neural, and Behavioral Physiology*. 1973; 85:235–266.
- Haag J, Borst A. Encoding of visual motion information and reliability in spiking and graded potential neurons. *Journal of Neuroscience*. 1997; 17:4809. [PubMed: 9169539]
- Harris R, O'Carroll D, Laughlin S. Adaptation and the temporal delay filter of fly motion detectors. *Vision Research*. 1999; 39:2603–2613. [PubMed: 10492824]

- Hassenstein B. Ommatidienraster und afferente Bewegungsintegration. *Journal of Comparative Physiology A: Neuroethology, Sensory, Neural, and Behavioral Physiology*. 1951; 33:301–326.
- Hassenstein B, Reichardt W. Systemtheoretische analyse der zeit-, reihenfolgenund vorzeichenauswertung bei der bewegungsperzeption des rüsselkäfers chlorophanus. *Zeitschrift für Naturforschung*. 1956; 11:513–524.
- Hateren J. Theoretical predictions of spatiotemporal receptive fields of fly LMCs, and experimental validation. *Journal of Comparative Physiology A: Neuroethology, Sensory, Neural, and Behavioral Physiology*. 1992; 171:157–170.
- Hausen K. Functional characterization and anatomical identification of motion sensitive neurons in the lobula plate of the blowfly *Calliphora erythrocephala*. *Z Naturforsch*. 1976; 31:629–633.
- Hausen K, Wehrhahn C. Neural circuits mediating visual flight control in flies. I. Quantitative comparison of neural and behavioral response characteristics. *Journal of Neuroscience*. 1989; 9:3828. [PubMed: 2585057]
- Hecht S, Wald G. The visual acuity and intensity discrimination of *Drosophila*. *The Journal of General Physiology*. 1934; 17:517. [PubMed: 19872798]
- Heisenberg M, Buchner E. The role of retinula cell types in visual behavior of *Drosophila melanogaster*. *Journal of Comparative Physiology A: Neuroethology, Sensory, Neural, and Behavioral Physiology*. 1977; 117:127–162.
- Hubel D, Wiesel T. Receptive fields and functional architecture of monkey striate cortex. *The Journal of Physiology*. 1968; 195:215. [PubMed: 4966457]
- Joesch M, Plett J, Borst A, Reiff D. Response properties of motion-sensitive visual interneurons in the lobula plate of *Drosophila melanogaster*. *Current Biology*. 2008; 18:368–374. [PubMed: 18328703]
- Joesch M, Schnell B, Raghu S, Reiff D, Borst A. ON and OFF pathways in *Drosophila* motion vision. *Nature*. 2010; 468:300–304. [PubMed: 21068841]
- Jones J, Palmer L. The two-dimensional spatial structure of simple receptive fields in cat striate cortex. *Journal of Neurophysiology*. 1987; 58:1187. [PubMed: 3437330]
- Juusola M, Uusitalo R, Weckström M. Transfer of graded potentials at the photoreceptor-interneuron synapse. *The Journal of General Physiology*. 1995; 105:117. [PubMed: 7537323]
- Kalmus H. Optomotor responses in *Drosophila* and *Musca*. *Physiologia comparata et oecologia; an international journal of comparative physiology and ecology*. 1949; 1:127.
- Katsov A, Clandinin T. Motion processing streams in *Drosophila* are behaviorally specialized. *Neuron*. 2008; 59:322–335. [PubMed: 18667159]
- Krekelberg B, Albright T. Motion mechanisms in macaque MT. *Journal of Neurophysiology*. 2005; 93:2908. [PubMed: 15574800]
- Laughlin S, Howard J, Blakeslee B. Synaptic limitations to contrast coding in the retina of the blowfly *Calliphora*. *Proceedings of the Royal society of London Series B Biological sciences*. 1987; 231:437.
- Laughlin S, Osorio D. Mechanisms for neural signal enhancement in the blowfly compound eye. *Journal of Experimental Biology*. 1989; 144:113–146.
- Livingstone M, Pack C, Born R. Two-dimensional substructure of MT receptive fields. *Neuron*. 2001; 30:781–793. [PubMed: 11430811]
- Mank M, Santos A, Drenth S, Mrcic-Flogel T, Hofer S, Stein V, Hendel T, Reiff D, Levelt C, Borst A. A genetically encoded calcium indicator for chronic in vivo two-photon imaging. *Nature Methods*. 2008; 5:805–811. [PubMed: 19160515]
- Marmarelis P, McCann G. Development and application of white-noise modeling techniques for studies of insect visual nervous system. *Biological Cybernetics*. 1973; 12:74–89.
- Mo CH, Koch C. Modeling reverse-phi motion-selective neurons in cortex: double synaptic-veto mechanism. *Neural computation*. 2003; 15:735–759. [PubMed: 12689385]
- Nordström K, O'Carroll DC. Feature detection and the hypercomplex property in insects. *Trends in neurosciences*. 2009; 32:383–391. [PubMed: 19541374]
- Reichardt W. Autocorrelation, a principle for relative movement discrimination by the central nervous system. *Sensory communication*. 1961:303–317.

- Reichardt W, Poggio T. Visual control of orientation behaviour in the fly: Part I. A quantitative analysis. *Quarterly Reviews of Biophysics*. 1976; 9:311–375. [PubMed: 790441]
- Reiff D, Plett J, Mank M, Griesbeck O, Borst A. Visualizing retinotopic half-wave rectified input to the motion detection circuitry of *Drosophila*. *Nature Neuroscience*. 2010; 13:973–978.
- Rister J, Pauls D, Schnell B, Ting C, Lee C, Sinakevitch I, Morante J, Strausfeld N, Ito K, Heisenberg M. Dissection of the peripheral motion channel in the visual system of *Drosophila melanogaster*. *Neuron*. 2007; 56:155–170. [PubMed: 17920022]
- Rodrigues V, Buchner E. [3H] 2-Deoxyglucose mapping of odor-induced neuronal activity in the antennal lobes of *Drosophila melanogaster*. *Brain research*. 1984; 324:374–378. [PubMed: 6442179]
- Sakai H, Ken-Ichi N, Korenberg M. White-noise analysis in visual neuroscience. *Visual Neuroscience*. 1988; 1:287–296. [PubMed: 3154801]
- Schiller PH, Finlay BL, Volman SF. Quantitative studies of single-cell properties in monkey striate cortex. I. Spatiotemporal organization of receptive fields. *Journal of Neurophysiology*. 1976; 39:1288. [PubMed: 825621]
- Seelig J, Chiappe M, Lott G, Dutta A, Osborne J, Reiser M, Jayaraman V. Two-photon calcium imaging from head-fixed *Drosophila* during optomotor walking behavior. *Nature Methods*. 2010
- Stavenga D. Angular and spectral sensitivity of fly photoreceptors. II. Dependence on facet lens F-number and rhabdomere type in *Drosophila*. *Journal of Comparative Physiology A: Neuroethology, Sensory, Neural, and Behavioral Physiology*. 2003; 189:189–202.
- Tammero L, Frye M, Dickinson M. Spatial organization of visuomotor reflexes in *Drosophila*. *Journal of Experimental Biology*. 2004; 207:113–122. [PubMed: 14638838]
- Theobald J, Ringach D, Frye M. Dynamics of optomotor responses in *Drosophila* to perturbations in optic flow. *J Exp Biol*. 2010; 213:1366–1375. [PubMed: 20348349]
- Van Hateren J, Kern R, Schwerdtfeger G, Egelhaaf M. Function and coding in the blowfly H1 neuron during naturalistic optic flow. *Journal of Neuroscience*. 2005; 25:4343. [PubMed: 15858060]
- Wiederman SD, Shoemaker PA, O'Carroll DC. A model for the detection of moving targets in visual clutter inspired by insect physiology. *PloS one*. 2008; 3:e2784. [PubMed: 18665213]
- Zhu Y, Nern A, Zipursky S, Frye M. Peripheral visual circuits functionally segregate motion and phototaxis behaviors in the fly. *Current Biology*. 2009; 19:613–619. [PubMed: 19303299]

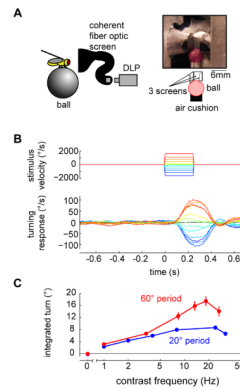


Figure 1. Fly behavior can be characterized by a fly's rotational response to visual stimuli while walking on a ball

(A) Left: Schematic illustration of a fly walking on a ball, viewing a small screen. The fly is suspended over the ball, which floats on an airstream. Each screen is 4x4 mm. One screen is directly in front of the fly, while the other two are to the left and right, and the fly's head is at the center. Two optical mice (not shown) capture the movements of the ball. Right: photograph of our screen and ball setup. The diagram below schematizes the ball surrounded by 3 screens. The fly is placed between the screens, above the ball. (B) Flies were subjected to the rotation of a virtual cylinder of 60° period square waves moving at varying speed (top traces denote cylinder speed). In response to brief pulses of rotation, flies produced the turning responses shown (bottom traces, color coded to match the top traces). (C) Integrating those curves from 80 ms after stimulus onset to 80ms after stimulus offset, we found that flies respond to increasing temporal contrast frequency with a characteristic increase and a fall-off at high frequencies. This was found at both spatial frequencies tested. N=8 and 14 for the 60 and 20 degree period square waves. ; error bars are \pm 1SEM, and can be smaller than the corresponding marker. (See Figure S1.)

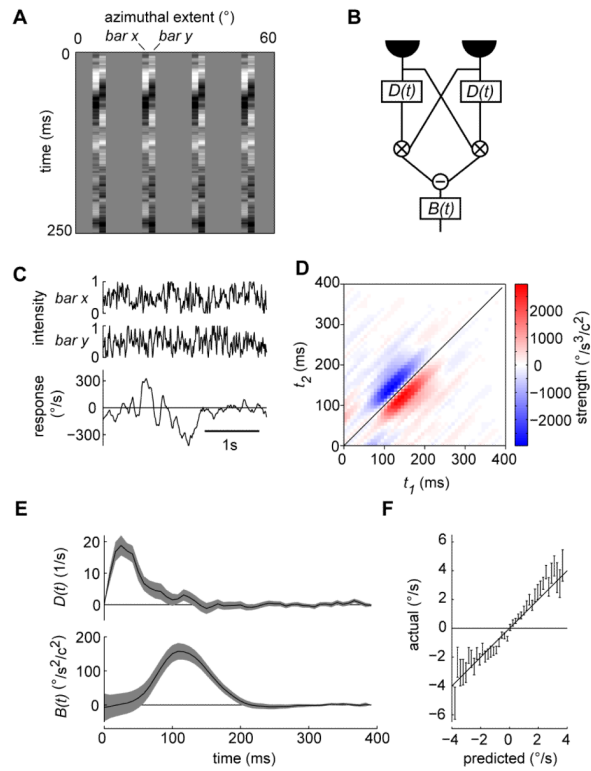


Figure 2. Characterizing *Drosophila*'s motion detector

(A) A space-time plot of a random bar pair stimulus in which individual bars in a pair update their intensities independently. Each bar is 2° in azimuthal extent, the bar pairs repeat every 15° , and the screens' vertical extent was approximately 80° . (B) The canonical model of spatio-temporal correlation proposed by Hassenstein and Reichardt. Intensities at one point in time are correlated with intensities at a neighboring point and subsequent time in order to extract motion information from a visual scene. The delay filter, $D(t)$, determines the relative temporal correlations considered by the detector. We have added a behavioral filter, $B(t)$, to account for the dynamics of the behavioral response. (C) Traces of the intensities of each bar (top) and an example of a fly's turning response to that stimulus (bottom). (D) A filter that best predicted the flies' responses given the two inputs (see Supplementary Methods). The flies did not react to the contrasts of the bars individually, but did respond to correlated intensities between the bars delayed by 20 to 30 ms ($N=48$ flies). In the filter units here and in (E), 'c' refers to the fractional bar contrast deviation from the mean. (E) The two dimensional filter can be used to fit the shape of the delay filter, $D(t)$ (top), and the behavioral response to motion detection, $B(t)$ (bottom), in the HRC shown in (B). The shaded areas represent ± 1 SEM. (F) A comparison of actual turning responses as a function of responses predicted by the filters in (E). The error bars represent ± 1 SEM. This comparison reveals a linear relationship. (See Figure S2.)

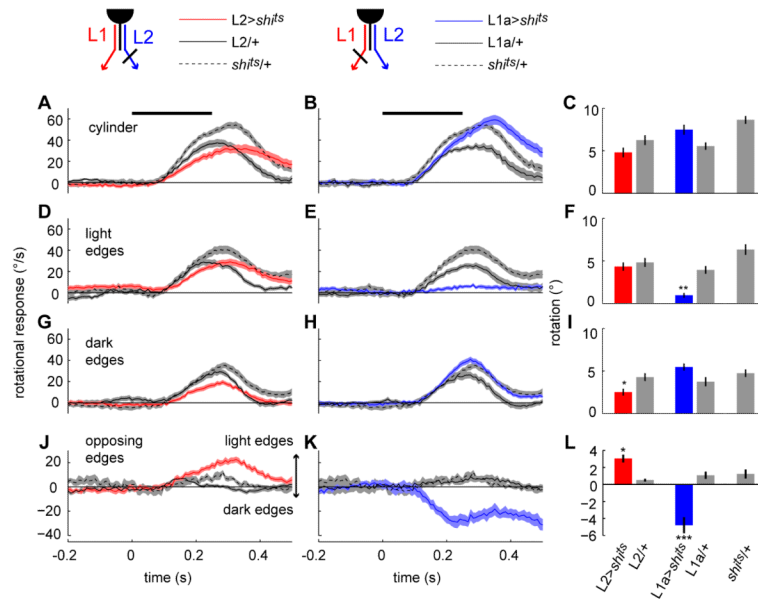


Figure 3. The L1- and L2-pathways mediate selective responses to specific moving edge polarities Plots of turning response as a function of time, evoked by four stimuli comprising different combinations of light and dark edges. The first row consists of responses to cylinders comprising a square wave grating, in which light and dark edges move in the same direction simultaneously. The second row consists of responses to light edges only, rotating about the fly. The third row consists of responses to dark edges only. The fourth row consists of responses to a stimulus in which light and dark edges rotate in opposite directions (see Figure S3A). (A, D, G, J) L1 pathway active. (B, E, H, K) L2 pathway active. (C, F, I, L) Integrated turning response of each genotype. Experimental curves are denoted in red (for the L1 pathway) and blue (for the L2 pathway); control genotypes are in gray. In (C,F,I), N for each genotype, left to right, is 25, 11, 23, 13, and 18. In (L), N for each genotype, left to right, is 12, 12, 6, 6, and 6. Shading and error bars here and in all subsequent figures represent ± 1 SEM. (*) denotes $P < 0.05$, (**) $P < 0.01$, and (***) $P < 0.001$ by a 2-tailed Student t-test compared to both controls. The thick black line in (A) and (B) denotes the period of stimulus motion. Here, and elsewhere, we observed that *UAS shits/+* controls behaved more robustly than other controls. (See Figure S3.)

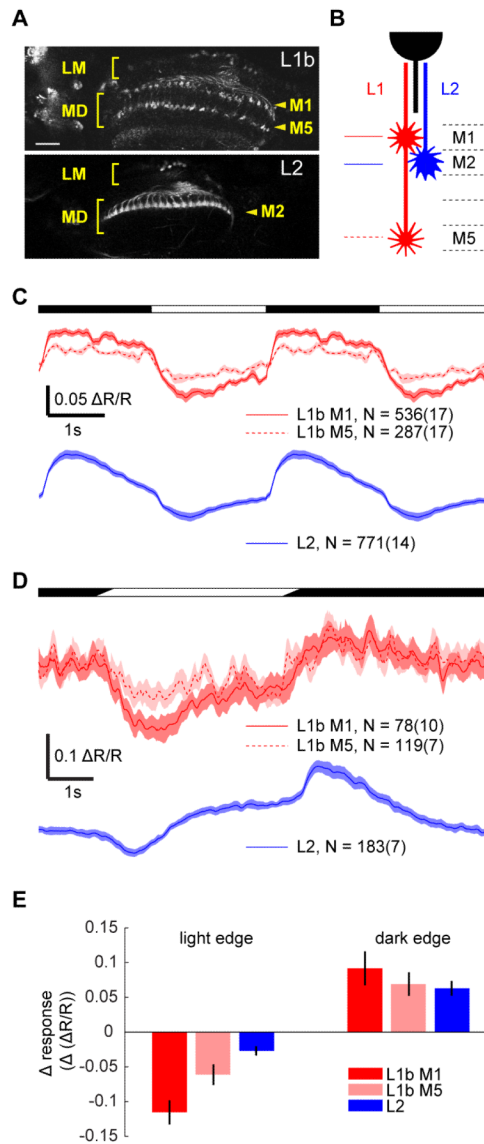


Figure 4. L1 and L2 axon terminals show similar responses to light steps and moving edges (A) Axonal morphologies of L1 (upper panel) and L2 (lower panel), using two photon imaging of TN-XXL expression. LM – lamina. MD – medulla. L1 axons terminate in two medulla layers, M1 and M5, while L2 terminates in the M2 layer. Scale bar = 25 μ m. (B) Schematic representation of L1 and L2 projections. (C) Response ($\Delta R/R$) of L1 projections into the M1 and M5 layers (top) to periodic full-field light flashes, and L2 projections into the M2 layer (bottom). Two 4-second periods are shown. Light on epochs are denoted with open sections of the bar and light off epochs with dark sections. Shading denotes ± 1 SEM. Here and below, Ns for each genotype are given as number-of-cells(number-of-flies). (D) Responses of the three axon terminal types to a bright edge that moved across the field of view at 80 $^\circ$ /s, after which the screen is light for 4 seconds, before a dark edge passed at 80 $^\circ$ /s. Top L1 terminals in M1 and M5. Bottom: L2 terminals. Shading denotes ± 1 SEM. (E) The transient response to each edge type was quantified by subtracting the difference in mean response during the second before the edge passes from the 1 second after it passes. Mean and SEM are calculated by fly, from the traces shown in (D). (See Figure S4.)

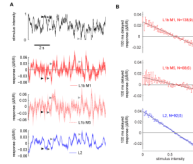


Figure 5. Calcium signals in L1 and L2 terminals respond linearly to dynamical light stimuli
(A) Top: a 10 second excerpt of the intensity signal in the full-field Gaussian noise stimulus. Middle: the corresponding average response observed in projections of L1 neurons into M1 (red) and M5 (red, dashed). Bottom: L2 axon terminals (blue). Shading denotes ± 1 SEM. Gray arrowheads in top panel mark peaks and troughs in the input; arrowheads in the middle and bottom panels mark the response to these peaks (which are inverted by the photoreceptor synapse). For each genotype N_s are given as number-of-cells(number-of-flies). **(B)** Calcium response as a function of intensity 100 ms earlier. The average response for each preceding intensity was computed for each fly, and the means and SEM of the fly means are displayed here. The black line is a linear fit to the means. (See Figure S5.)

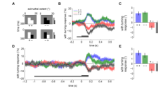


Figure 6. Wild-type flies respond to all four unit computations performed by the HRC
 (A) Space-time intensity plots of bar pairs that appear sequentially in time and space, either increasing or decreasing in intensity relative to the mean. (B,D) Time traces of the fly turning response to the four combinations of Reichardt bar pairs. The relative timing of the two bars is shown by the thick black lines at the bottom. The delay between bar changes in (B) is 100 ms, while it is 1 s in (D). (C,E) The total turn in response to each stimulus was determined by integrating the turning velocity over 250 ms, starting 80 ms after the second bar appeared. The data in (C) correspond to the traces in (B), while (E) corresponds to (D). N=13 for (B) and (C) and N=20 for (D) and (E).

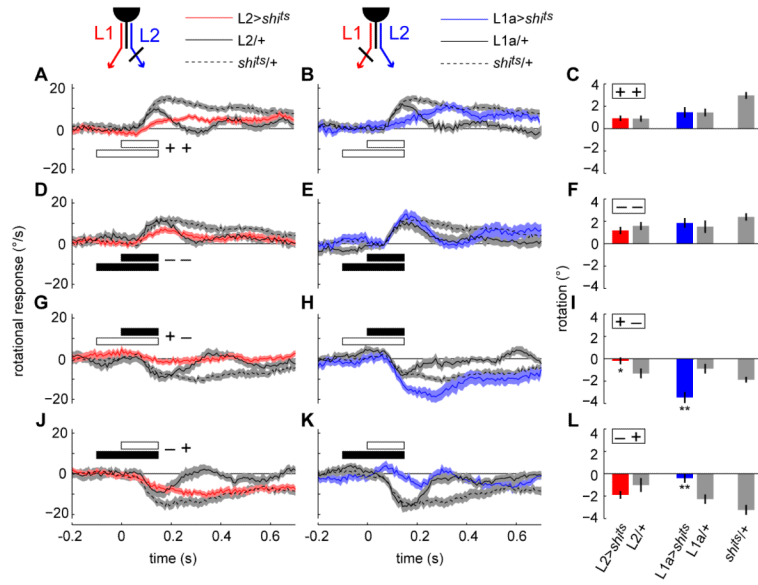


Figure 7. L1- and L2-silenced flies respond differentially to sequential bar pairs

Plots of turning responses as a function of time to four different minimal motion stimuli, corresponding to sequential brightening (A-C, two open bars, denoted + +), sequential darkening (D-F, two black bars, denoted - -), bright-dark reverse phi (G-I, open bar before black bar, denoted + -), and dark-bright reverse phi (J-L, black bar before open bar, denoted - +). The left-hand column shows the L1-pathway, where the red coloring indicates that L2 has been silenced. The middle column, in blue, shows the complementary silencing of the L1-pathway. (C,F,I,L) Each genotype's response to the set of 4 pairs was quantified by examining the integrated responses. (*) denotes $P < 0.05$ by a two-tailed Student t-test to both controls, while (**) denotes $P < 0.01$. N for each genotype, left to right in the bar plots, is 36, 18, 20, 17, and 24. (See Figure S6.)

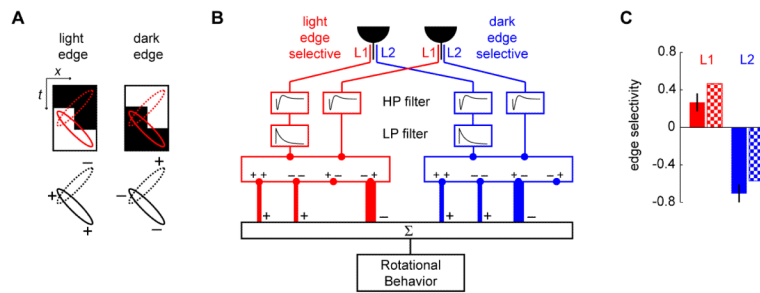


Figure 8. A model of edge selectivity through differential weighting of HRC unit computations (A) Schematic space-time illustration of an edge passing through the field of view of an elementary motion detector. Both phi (solid oval) and reverse phi (dashed oval) correlation pairs are present in the stimulus, but each reverse phi is associated with only one edge type. (B) A weighted quadrant model: architecture of the two input pathways and weighting (line thickness) of the HRC outputs constructed to match the behavioral observations in L1- and L2-silenced flies. Inputs are filtered before being split into four multiplication steps, which are weighted differently in the two pathways. Turning behavior is guided by the summed outputs of both pathways. For simplicity, only one half of the correlators are shown (see Figure S1B). (C) Edge selectivity of the L1 and L2 pathways, observed by experiment, and predicted by the model. Edge selectivity is defined as the integrated light edge turning response minus the integrated dark edge turning response, divided by their sum. The measured selectivity is shown by the solid bars (mean \pm 1 SEM, data from Figure 3), while the modeled selectivity is shown by the checkered bars. (See Figure S7.)